PCCP

PAPER

View Article Online
View Journal | View Issue

Cite this: *Phys. Chem. Chem. Phys.*, 2019, **21**, 16353

Delayed photoacidity produced through the triplet–triplet annihilation of a neutral pyranine derivative†

J. Christian Lennox,[a] Evgeny O. Danilov[b] and Jillian L. Dempsey *[a]

Received 24th May 2019,
Accepted 8th July 2019

DOI: 10.1039/c9cp02929j

rsc.li/pccp

A novel pyranine derivative, ^{Et}HPTA-OH, was synthesized *via* the substitution of the anionic sulfonate groups with neutral diethylsulfonamide groups. The photophysical and photochemical properties of ^{Et}HPTA-OH were studied using photoluminescence quenching and transient absorption spectroscopy. The singlet state of ^{Et}HPTA-OH was found to be highly photoacidic (pK_a^* = 8.74 in acetonitrile). A series of aniline and pyridine bases were used to investigate excited-state proton transfer (ESPT) from singlet ^{Et}HPTA-OH, and rate constants for singlet quenching *via* ESPT were determined (k_q = 5.18 × 10^9 to 1.05 × 10^{10} M^{-1} s^{-1}). ^{Et}HPTA-OH was also found to exhibit a long-lived triplet state which reacts through a triplet–triplet annihilation (TTA) process to reform singlet ^{Et}HPTA-OH on timescales of up to 80 μs. Detection of ESPT photoproducts on timescales comparable to that of TTA singlet regeneration provides strong evidence for photoacidic behavior stemming from the regenerated singlet ^{Et}HPTA-OH.

Introduction

The excitation of photoacids produces powerful proton donors that can trigger proton-coupled electron transfer (PCET) reactions. Coupled to time-resolved optical measurements, photoacids are poised to be a powerful tool for the study of PCET reaction mechanisms. However, to our knowledge, only one photoacid-initiated PCET reaction has been reported in the literature.[1,2] This lies in stark contrast to the countless examples where PCET reactions are initiated by a phototriggered electron transfer reaction.[3–13] This difference can partly be blamed on a dearth of well-behaved photoacids (and photobases) in comparison to the plethora of known photo-reductants and photo-oxidants. An ideal photoacid exhibits (1) absorption bands in the visible region to enable selective visible light excitation, (2) a long-lived excited state to allow for intermolecular reactions, (3) reversible photochemistry, (4) a large reduction in pK_a upon excitation, and (5) good solubility in both water and organic solvents to allow for the facile study of excited-state proton transfer (ESPT) in both protic and aprotic media. Few photoacids meet these criteria, making the study of photoacid-driven PCET reactions difficult.

Pyranines are one promising class of photoacids for application in the study of PCET reactions. The photoacidic properties of unsubstituted pyranine (Scheme 1) are well understood[14–21] and it has found broad use in biological systems due to its strong fluorescence, high aqueous solubility, and low toxicity. Like most hydroxyarene photoacids, pyranine and pyranine-derived photoacids exhibit reversible photochemistry, and several derivatives have been reported to exhibit visible absorption bands and large ΔpK_a values ($\Delta pK_a > -6$ in water, where $\Delta pK_a = pK_a^* - pK_a$).[22,23]

Substitution of the sulfate groups of pyranine with more electron-withdrawing sulfonamide groups has been shown to enhance the photoacidity (increase ΔpK_a) of the photoacid,[24] but these sulfonamide derivatives have not seen widespread adoption as photoacids and for this reason their photophysics and photochemistry are not well understood. The limited

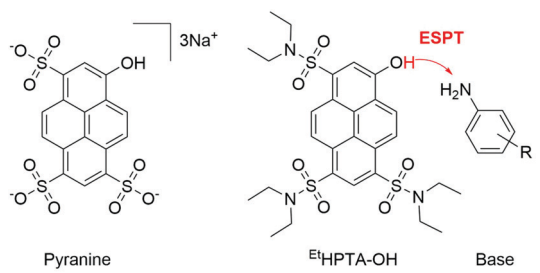

Scheme 1 Pyranine and N^1,N^1,N^3,N^3,N^6,N^6-hexaethyl-8-hydroxypyrene-1,3,6-trisulfonamide (^{Et}HPTA-OH) with example of excited-state proton transfer.

[a] *Department of Chemistry, University of North Carolina, Chapel Hill, North Carolina, USA 27599. E-mail: dempseyj@email.unc.edu*
[b] *Department of Chemistry, North Carolina State University, Raleigh, North Carolina, USA 27695*

† Electronic supplementary information (ESI) available. See DOI: 10.1039/c9cp02929j

number of studies involving the neutral sulfonamide derivatives most likely stems from perceived barriers to their synthesis; most reported syntheses access the target photoacids *via* schemes that involve aqueous amines. Under these conditions, water can quench the reactive sulfonyl chloride intermediate and reverses the reaction, reforming the sulfate and leading to poor yields.[22] Our lab has recently developed a simplified synthetic route to neutral sulfonamide derivatives, and has prepared a novel pyranine derivative (N^1,N^1,N^3,N^3,N^6,N^6-hexaethyl-8-hydroxypyrene-1,3,6-trisulfonamide, ^{Et}HPTA-OH) where the sulfate groups of the parent pyranine have been substituted with diethylsulfonamide moieties. ^{Et}HPTA-OH displays good solubility in both water and organic solvents, allowing comprehensive characterization of its photophysics and the proton transfer reactivity of the singlet excited state on the nanosecond timescale. Excitingly, we discovered that ^{Et}HPTA-OH also reacts on the microsecond timescale through a strongly photo-acidic singlet state that is populated from a triplet state through a triplet–triplet annihilation mechanism. These findings deeply enhance our understanding of the photophysics and photochemistry of neutral sulfonamide-derivatized pyranines and lay key groundwork for application of ^{Et}HPTA-OH for the study of PCET reactions.

Results and discussion

Synthesis of ^{Et}HPTA-OH

This pyranine derivative was readily produced through a three-step synthesis in which trisodium 8-hydroxypyrene-1,3,6-trisulfate (pyranine) was protected *via* acetylation and then refluxed in thionyl chloride to yield the tris(chlorosulfonyl) intermediate, which was immediately reacted with an excess of diethylamine to yield N^1,N^1,N^3,N^3,N^6,N^6-hexaethyl-8-hydroxypyrene-1,3,6-trisulfonamide (^{Et}HPTA-OH) following deprotection (Scheme 2).[22] The use of anhydrous diethylamine – a neat liquid – circumvents the use aqueous amine solutions typically found in comparable syntheses. Furthermore, as diethylamine functions both as a nucleophile and a base, no additional base is required in the synthesis.

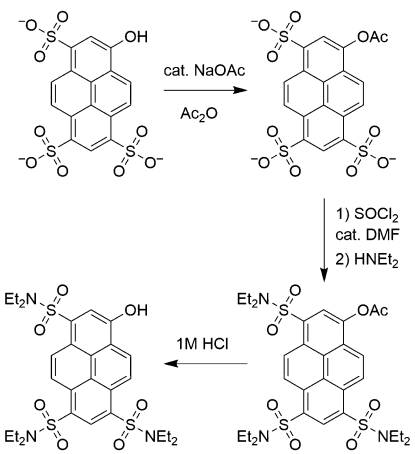

Scheme 2 Synthetic route from pyranine to ^{Et}HPTA-OH.

Characterization of ^{Et}HPTA-OH

^{Et}HPTA-OH displays marked differences in absorbance depending on its protonation state (Fig. 1). In acetonitrile, the absorbance and emission spectra of the protonated photoacid displays structured features in the visible region ($\lambda_{max,abs}$ = 419 nm, ε = 31 200 M^{-1} cm^{-1}; $\lambda_{max,PL}$ = 447 nm, Φ_{PL} = 0.51). The 2.90 ns luminescence lifetime along with the small Stokes shift between the absorbance and emission maxima support assignment of the luminescence as originating from the singlet state. In the steady-state photoluminescence spectrum, the emission profile contains two overlapping features, corresponding to relaxation from the ^1L_b state at 447 nm and the ^1L_a state at 470 nm (Fig. 2). In the parent pyranine, the ^1L_a state contains more charge transfer character, wherein electron density moves from the hydroxyl group into the aromatic ring system, resulting in a more strongly photoacidic excited state.[19,25] Assignment of these excited states in ^{Et}HPTA-OH are made by comparison to the structured emission bands reported for both pyranine and other similar pyranine derivatives, and are supported *via* solvatochromism studies in dichloromethane (Fig. S1, ESI†) which show the disproportionate enhancement of emission from the ^1L_a state upon addition of a polar, hydrogen-bonding solvent (acetonitrile), consistent with literature reports of solvent-dependent emission enhancement in pyranine and other pyranine sulfonamide derivatives.[19,25] Upon deprotonation to form ^{Et}HPTA-O$^-$, both absorbance and emission λ_{max} shift bathochromically, the Stokes shift decreases, the extinction coefficient increases by more than a factor of two, and the quantum yield increases by 30% (λ_{abs} = 548 nm, ε = 75 500 M^{-1} cm^{-1}, λ_{PL} = 568 nm Φ_{PL} = 0.65). Of note, photoluminescence dilution experiments showed no evidence for excimer formation.

Spectrophotometric titrations of ^{Et}HPTA-OH in acetonitrile using *N*,*N*-dimethylpyridin-4-amine (DMAP) were used to determine the ground-state pK_a of ^{Et}HPTA-OH (19.52) (Fig. S2, ESI†).

The energy stored in the singlet excited state (E_{00}) was approximated for ^{Et}HPTA-OH (2.86 eV) and ^{Et}HPTA-O$^-$ (2.22 eV) from the intersection of the normalized absorption and emission spectra of the two species (Fig. S3, ESI†). From these two values,

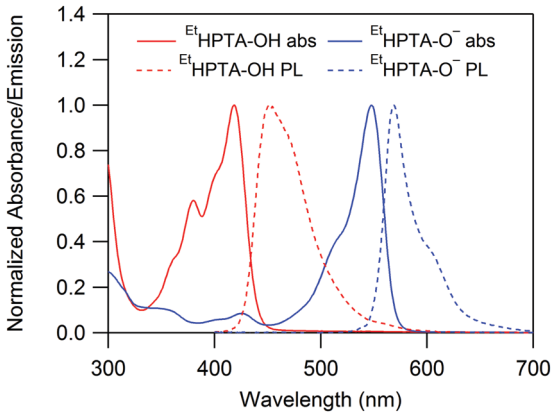

Fig. 1 Normalized absorbance and photoluminescence spectra of ^{Et}HPTA-OH and ^{Et}HPTA-O$^-$ in acetonitrile.

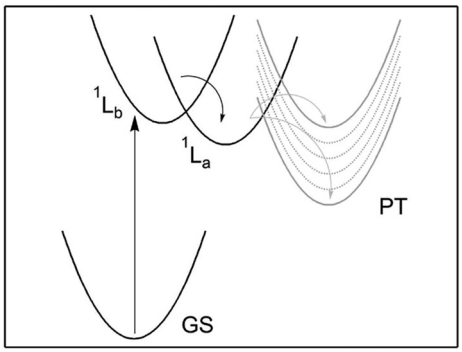

Fig. 2 Schematic representation of the ^1L_b and ^1L_a singlet excited states of pyranine photoacids, as well as the final proton transfer state. Direct excitation into the ^1L_b state is followed by interconversion to the ^1L_a state which is promoted by polar and H-bonding solvents. The ^1L_a state is more strongly photoacidic and yields the final proton transfer state in the presence of base. A variety of minima are depicted for the PT state, reflecting exergonic and endergonic PT to stronger and weaker bases, respectively.

along with the ground state pK_a of ^{Et}HPTA-OH, a Förster cycle can be constructed to approximate the pK_a of the singlet excited state of ^{Et}HPTA-OH (Scheme 3). This analysis indicates the excited state is *ca.* 11 units stronger than the ground state (^{1}pK_a* = 8.74).

Singlet excited state photophysics and photochemistry of ^{Et}HPTA-OH

A series of aniline and pyridine bases with a range of pK_a values (7.0–14.1 in acetonitrile, Table 1) bookending the ^{1}pK_a* of ^{Et}HPTA-OH were selected to test the excited-state proton transfer reactivity of ^{Et}HPTA-OH in acetonitrile. Reduction in the intensity of steady-state photoluminescence of ^{Et}HPTA-OH upon the addition of base was observed, consistent with quenching *via* ESPT. However, analysis of the steady-state photoluminescence data was complicated by strong enhancement of the ^1L_a band and moderate enhancement of the ^1L_b band upon addition of hydrogen bond acceptors and increased solvent dielectric constant (see solvatochromism study, Fig. S1, ESI†).[19,25] As such, the change in luminescence intensity upon addition of base is a convolution of excited-state quenching *via* ESPT, luminescence enhancement *via* hydrogen bonding, and luminescence enhancement or attenuation

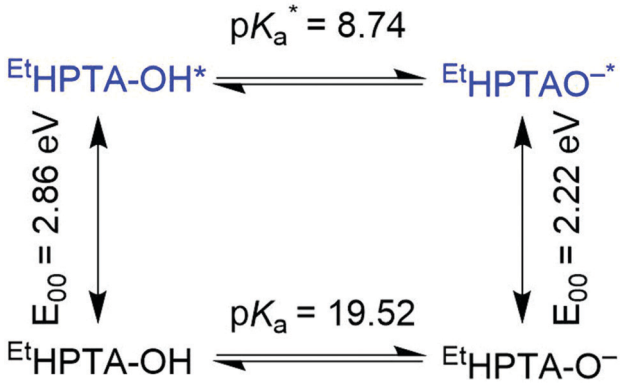

Scheme 3 Förster cycle of ^{Et}HPTA-OH.

due to changes in bulk solvent polarity. Furthermore, due to the spectral overlap of the ^1L_a and ^1L_b emission bands, as well as the greater influence of the above factors on the ^1L_a decay, Gaussian deconvolution was necessary to resolve the emission from each state, and Stern–Volmer plots of emission quenching from each state yield different slopes due to the contrast in sensitivity of each state to hydrogen bonding and polarity (Fig. S4–S10, ESI†). Due to these complications, an accurate quantitative measurement of the Stern–Volmer quenching constant was not possible through steady-state measurements. However, valuable qualitative observations can still be made: no upwards curvature was found in the Stern–Volmer plots, the appearance of which would indicate the presence of both static and dynamic quenching with a given base.

Assignment of an ESPT mechanism for the quenching of ^{Et}HPTA-OH luminescence is supported by the observation of ^{Et}HPTA-O$^-$ emission at 568 nm in samples with base present. This observation is most diagnostic of ESPT for samples with weak bases in which no appreciable quantities of ^{Et}HPTA-O$^-$ are produced *via* ground state acid–base equilibrium.[23,25,26] For instance, at the highest concentrations (30 mM) of 4-cyanoaniline (pK_a (BH$^+$) = 7) used, samples with ^{Et}HPTA-OH (50 μM, pK_a = 19.52), the ground-state proton transfer equilibrium constant (K_{eq} = 1.61 × 10^{-13}) predicts a concentration of ^{Et}HPTA-O$^-$ of 0.50 nM. However, under these conditions, emission is detected at 568 nm, which is not present in samples without base, consistent with emission from the deprotonated photoacid following ESPT. Under similar conditions with stronger bases, these observations qualitatively hold, although contributions from ^{Et}HPTA-O$^-$ become relevant as the strength of the base increases.

Due to the above limitations in the analysis of steady-state photoluminescence quenching of ^{Et}HPTA-OH, time-correlated single photon counting (TCSPC) was used to further investigate ESPT from ^{1}*[^{Et}HPTA-OH] in the presence of base. Upon addition of monoquat (MQ$^+$) or aniline bases, the singlet lifetime of ^{Et}HPTA-OH is attenuated, consistent with diffusional quenching *via* ESPT from ^{Et}HPTA-OH to the added base (Fig. 3 and Fig. S11–S14, ESI†). Rate constants for the quenching of ^{Et}HPTA-OH luminescence were obtained through Stern–Volmer analysis (Table 1), which reveal a slight correlation between quenching rate constants and base strength ($\delta\log(k_q)/\delta pK_a = 0.066$). Addition of pyridine or 2,6-lutidine produces no attenuation of the singlet lifetime of ^{Et}HPTA-OH, indicating no dynamic quenching for these bases (Fig. S15 and S16, ESI†). However, quenching of ^{Et}HPTA-OH photoluminescence in the presence of these bases was observed in steady-state measurements (above). For these reasons, we assign a static quenching mechanism for the reactivity of ^{1}*[^{Et}HPTA-OH] with these bases. The underlying cause of the difference in quenching mechanism between MQ$^+$ and aniline bases (dynamic quenching bases) and the neutral pyridines (static quenching bases) is not immediately apparent. We hypothesize that reactivity differences may arise from relative hydrogen bond strengths. Broadly, anilines are weaker hydrogen bond acceptors than pyridine bases, and are weaker hydrogen bond acceptors than they are hydrogen bond donors.[27] Aniline bases engaged in hydrogen bonding with the

Table 1 pK_a(CH_3CN) values of bases used and rate constants for the quenching of ^{1}*[^{Et}HPTA-OH] (M^{-1} s^{-1}) determined *via* Stern–Volmer analysis of time-resolved luminescence quenching

Base	^{4}CN-An[a]	^{4}Br-An[b]	MQ^+	An[c]	^{4}MeO-An[d]	Pyridine	Lutidine
pK_a	7.0	9.43	10.4	10.62	11.86	12.56	14.13
k_q	5.18×10^9	8.33×10^9	9.08×10^9	1.05×10^{10}	1.03×10^{10}	—	—

[a] 4-Cyanoaniline. [b] 4-Bromoanline. [c] Aniline. [d] 4-Methoxyaniline.

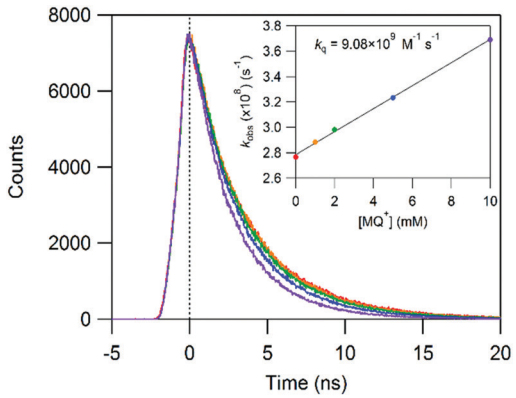

Fig. 3 Quenching of ^{Et}HPTA-OH fluorescence at 480 nm by 0–10 mM MQ^+ in acetonitrile with 0.1 M [NBu_4][PF_6] as measured by TCSPC. Inset: Stern–Volmer analysis of quenching.

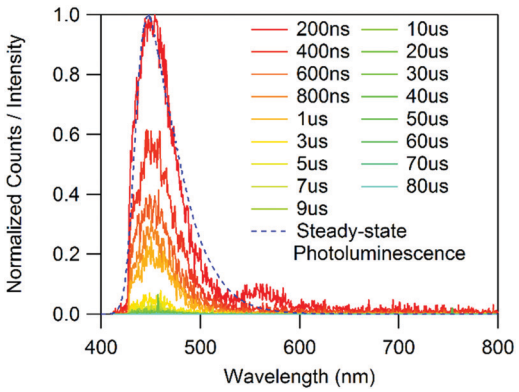

Fig. 4 Delayed fluorescence spectra of ^{Et}HPTA-OH collected at varying time delays following laser excitation (λ_{exc} = 419 nm) and normalized steady-state photoluminescence spectrum for comparison. 1 mM 2,4,6-collidinium tetrafluoroborate was added to protonate any trace ^{Et}HPTA-O^-. Samples prepared in 0.1 M [NBu_4][PF_6] acetonitrile solution.

hydroxyl group of ^{Et}HPTA-OH may act as hydrogen bond donors, with the oxygen of the hydroxyl group as the hydrogen bond acceptor, inhibiting an intra-adduct ESPT. Pyridine is a stronger hydrogen bond acceptor and does not also function as a hydrogen bond donor; intra-adduct ESPT in ^{Et}HPTA-OH···B occurs *via* a static quenching mechanism. The charge of MQ^+ compared to the neutral pyridines may give rise to the differences within this class of pyridine bases.

Triplet excited state photophysics and photochemistry of ^{Et}HPTA-OH

No phosphorescence was resolved in the steady-state emission measurements; to ascertain whether the high quantum yield (Φ_{PL} = 0.51) of the singlet state inhibited detection, we employed a time-gated ICCD camera to collect photoluminescence spectra at time delays well beyond the lifetime of ^{1}*[^{Et}HPTA-OH] (200 ns–80 μs delay after laser excitation, 250–500 ns gate). Emission was detected on long timescales (up to 80 μs, detector limited) with λ_{PL} centered at *ca.* 450 nm (Fig. 4). The high energy and long lifetime of this delayed emission in comparison to the prompt singlet PL observed *via* steady-state and TCSPC methods, suggests P-type delayed fluorescence from ^{Et}HPTA-OH.[19] While P-type fluorescence has not been reported for pyranines, their substituted-pyrene relatives, such as pyrene-1,3,6,8-tetrasulfate, are reported to display P-type delayed fluorescence at very high (>1 M) electrolyte concentrations, where the electrolyte can sufficiently screen the negative charge of the sulfonate groups and allow for triplet–triplet annihilation (TTA).[28] We hypothesize that the neutral sulfonamides groups on ^{Et}HPTA-OH allow for TTA and the regeneration of ^{1}*[^{Et}HPTA-OH] at low concentrations of electrolyte.

To assess the photoacidic reactivity of the triplet state of ^{Et}HPTA-OH, delayed fluorescence was measured in the presence of a proton acceptor (MQ^+). The lifetime of the delayed fluorescence is not attenuated upon the addition of MQ^+ (Fig. S17, ESI†). As the rate of regeneration of ^{1}*[^{Et}HPTA-OH] through TTA is determined solely by the concentration of ^{3}*[^{Et}HPTA-OH], this observation indicates that MQ^+ does not react with ^{3}*[^{Et}HPTA-OH] prior to TTA.[28]

To further verify that fluorescence quenching arises from an ESPT process, nanosecond transient absorption (TA) spectroscopy was used to detect the photoproducts of proton transfer. At moderate (1–30 mM) concentrations of the bases observed to undergo diffusional quenching (anilines and MQ^+), an unexpected biphasic growth of a transient species is observed at 548 nm, corresponding to the formation of the deprotonated photoacid, ^{Et}HPTA-O^- (Fig. S18–S22, ESI†). The anticipated prompt transient signal observed immediately after the laser pulse (5–7 ns FWHM) is attributed to ^{Et}HPTA-O^- generated through quenching of ^{1}*[^{Et}HPTA-OH] *via* ESPT to the added base. An unanticipated slow growth of the transient signal is observed on the 100 μs timescale; this longer timescale process is attributed to quenching of the ^{1}*[^{Et}HPTA-OH] generated through TTA and subsequent quenching *via* ESPT with added base, again producing ^{Et}HPTA-O^- and the conjugate acid (Scheme 4). Under pseudo-first order conditions (excess base), the growth of the transient feature fits to single exponential kinetics to yield a second-order observed rate constant $k_{g,obs}$ that spans a small range of values ($1.23–2.92 \times 10^6$ M^{-1} s^{-1}) across the MQ^+ and aniline bases (Table S1, ESI†). This observed rate constant for transient

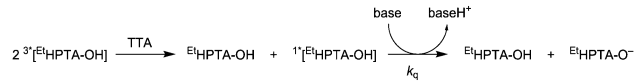

Scheme 4 Proposed pathway for the delayed production of ^{Et}HPTA-O$^-$.

growth is a convolution of the generation of ^{1}*[^{Et}HPTA-OH] through TTA and the subsequent diffusional quenching *via* ESPT. As expected, this observed rate constant ($k_{g,obs}$) trends with the rate constant for singlet quenching (k_q) but as the observed rate constant is also dependent on the preceding TTA reaction and thus also on the concentration of ^{3}*[^{Et}HPTA-OH], it is susceptible to other variance due to any deviation from our standard experimental conditions (*e.g.* fluctuations in laser power).

In samples containing the neutral pyridine bases, pyridine and 2,6-lutidine, only a prompt transient signal is observed at 548 nm, with no slow growth component (Fig. S23 and S24, ESI†). Instead, the transient signal observed at 548 nm decays immediately following the laser pulse. The absence of a slow transient growth is consistent with the observation that these bases undergo only static quenching and do not participate in diffusional quenching. Without diffusional quenching of the regenerated ^{1}*[^{Et}HPTA-OH], no further photoproducts form and back proton transfer is observed immediately.

Over hundreds of microseconds, decay of the ^{Et}HPTA-O$^-$ signal at 548 nm is observed for all samples containing base. Decay of the transient can be fit with second-order kinetics reflecting the exergonic back proton transfer between ground state ^{Et}HPTA-O$^-$ and the protonated base (ΔG° = −7.37 to −17.15 kcal mol^{-1}). Due to the presence of a small quantity of ^{Et}HPTA-O$^-$ (<1% of ^{Et}HPTA-OH) prior to irradiation resulting from basic impurities in acetonitrile, the concentrations of photogenerated ^{Et}HPTA-O$^-$ and protonated base are not precisely 1 : 1 in some samples and the kinetics for the decay cannot be fit to equal second-order concentrations kinetics. A kinetic model was constructed that accounts for the additional ^{Et}HPTA-O$^-$ using a differential equation solver. A series of differential equations describing the change in concentrations of reactants *versus* time were input to an ordinary differential equation solver in MATLAB along with the concentrations of the reactants at the beginning of the simulation, as obtained through ΔOD and ground-state absorbance measurements. Simulated TA traces with varied rate constants were generated until agreement was found with the experimental data (Fig. S25–S31, ESI†). Full details of the kinetics model can be found in the ESI.† As expected for exergonic back proton transfer (ΔG° = −7.37 to −17.2 kcal mol^{-1}), all rate constants were found to be near the diffusion limit in acetonitrile (k_{BPT} = 4.7 × 10^9 to 1.9 × 10^{10} M^{-1} s^{-1}).

Conclusions

In conclusion, we have found novel reactivity in a new derivative of pyranine wherein a photoacidic singlet state is regenerated through a TTA mechanism, enabled through the replacement of the anionic sulfate groups of the native pyranine with neutral diethylsulfonamide moieties. To our knowledge, there have been no reports of this mechanism of delayed photoacidity, although the prompt singlet reactivity of other neutral sulfonamide derivatives of pyranine has been previously studied.[24,25,29] This exciting reactivity warrants investigation into new systems to able to harness it to leverage interesting and productive chemistry. Ideally, neutral sulfonamide pyranine derivatives such as ^{Et}HPTA-OH will prove useful in the study of photoacid-initiated PCET, an underexplored area of research that merits further investigation.

Conflicts of interest

There are no conflicts to declare.

Acknowledgements

This work was supported by the National Science Foundation (CHE-1452615). We thank Dan Kurtz for helpful discussions, Carolyn Hartley for experimental assistance, and Felix Castellano assistance in obtaining time-gated photoluminescence spectra. We thank the University of North Carolina's Department of Chemistry Mass Spectrometry Core Laboratory, especially Brandie Ehrmann, for their assistance with mass spectrometry analysis. Instrumentation in the Mass Spectrometery Core Laboratory is supported by the National Science Foundation (CHE-1726291).

Notes and references

1 J. C. Lennox, D. A. Kurtz, T. Huang and J. L. Dempsey, *ACS Energy Lett.*, 2017, **2**, 1246–1256.
2 J. L. Dempsey, J. R. Winkler and H. B. Gray, *J. Am. Chem. Soc.*, 2010, **132**, 16774–16776.
3 S. Y. Reece and D. G. Nocera, *J. Am. Chem. Soc.*, 2005, **127**, 9448–9458.
4 T. Irebo, S. Y. Reece, M. Sjödin, D. G. Nocera and L. Hammarström, *J. Am. Chem. Soc.*, 2007, **129**, 15462–15464.
5 S. Y. Reece, M. R. Seyedsayamdost, J. Stubbe and D. G. Nocera, *J. Am. Chem. Soc.*, 2007, **129**, 13828–13830.
6 A. A. Pizano, J. L. Yang and D. G. Nocera, *Chem. Sci.*, 2012, **3**, 2457–2461.
7 M. Kuss-Petermann, H. Wolf, D. Stalke and O. S. Wenger, *J. Am. Chem. Soc.*, 2012, **134**, 12844–12854.
8 W. Herzog, C. Bronner, S. Löffler, B. He, D. Kratzert, D. Stalke, A. Hauser and O. S. Wenger, *ChemPhysChem*, 2013, **14**, 1168–1176.
9 C. Bronner and O. S. Wenger, *Phys. Chem. Chem. Phys.*, 2014, **16**, 3617–3622.
10 J. Chen, M. Kuss-Petermann and O. S. Wenger, *Chem. – Eur. J.*, 2014, **20**, 4098–4104.
11 M. Kuss-Petermann and O. S. Wenger, *J. Phys. Chem. A*, 2013, **117**, 5726–5733.
12 L. A. Büldt, A. Prescimone, M. Neuburger and O. S. Wenger, *Eur. J. Inorg. Chem.*, 2015, 4666–4677.

13 K. T. Tarantino, P. Liu and R. R. Knowles, *J. Am. Chem. Soc.*, 2013, **135**, 10022–10025.
14 E. Tietze and O. Bayer, *Justus Liebigs Ann. Chem.*, 1939, **540**, 189–210.
15 K. Kano and J. H. Fendler, *Biochim. Biophys. Acta, Biomembr.*, 1978, **509**, 289–299.
16 N. R. Clement and J. M. Gould, *Biochemistry*, 1981, **20**, 1534–1538.
17 R. M. Straubinger, D. Papahadjopoulos and K. Hong, *Biochemistry*, 1990, **29**, 4929–4939.
18 N. Barrash-Shiftan, B. Brauer and E. Pines, *J. Phys. Org. Chem.*, 1998, **11**, 743–750.
19 T.-H. Tran-Thi, C. Prayer, P. Millié, P. Uznanski and J. T. Hynes, *J. Phys. Chem. A*, 2002, **106**, 2244–2255.
20 D. B. Spry, A. Goun and M. D. Fayer, *J. Phys. Chem. A*, 2007, **111**, 230–237.
21 C. Spies, B. Finkler, N. Acar and G. Jung, *Phys. Chem. Chem. Phys.*, 2013, **15**, 19893–19905.
22 B. Finkler, C. Spies, M. Vester, F. Walte, K. Omlor, I. Riemann, M. Zimmer, F. Stracke, M. Gerhards and G. Jung, *Photochem. Photobiol. Sci.*, 2014, **13**, 548–562.
23 L. M. Tolbert and K. M. Solntsev, *Acc. Chem. Res.*, 2002, **35**, 19–27.
24 D. B. Spry and M. D. Fayer, *J. Chem. Phys.*, 2008, **128**, 084508.
25 D. B. Spry and M. D. Fayer, *J. Chem. Phys.*, 2007, **127**, 204501.
26 B.-Z. Magnes, N. V. Strashnikova and E. Pines, *Isr. J. Chem.*, 1999, **39**, 361–373.
27 W. K. Stephenson and R. Fuchs, *Can. J. Chem.*, 1985, **63**, 2540–2544.
28 C. Bohne, E. B. Abuin and J. C. Scaiano, *J. Am. Chem. Soc.*, 1990, **112**, 4226–4231.
29 E. Pines, D. Pines, Y. Ma and G. R. Fleming, *ChemPhysChem*, 2004, **5**, 1315–1327.

